e-Print: 2104.05769 [hep-ex]
Report number: FERMILAB-PUB-21-181-ND

Prepared for submission to JINST

Use of Neutrino Scattering Events with Low Hadronic Recoil to Inform Neutrino Flux and Detector Energy Scale

The MINERνA Collaboration

A. Bashyal[a] **D. Rimal**[b] **B. Messerly**[c] **Z. Ahmad Dar**[d,e] **F. Akbar**[e] **M. V. Ascencio**[f] **A. Bercellie**[g] **M. Betancourt**[h] **A. Bodek**[g] **J. L. Bonilla**[k] **A. Bravar**[i] **H. Budd**[g] **G. Caceres**[j] **T. Cai**[g] **H. da Motta**[j] **S.A. Dytman**[c] **G.A. Díaz** [g] **J. Felix**[k] **L. Fields**[l,h] **A. Filkins**[d] **R. Fine**[g] **A.M. Gago**[f] **A. Ghosh**[m,j] **S. Gilligan**[a] **D.A. Harris**[n,h] **S. Henry**[g] **S. Jena**[o] **D. Jena**[h] **J. Kleykamp**[g] **M. Kordosky**[d] **D. Last**[p] **A. Lozano**[j] **X.-G. Lu**[q] **E. Maher**[r] **S. Manly**[g] **W.A. Mann**[s] **C. Mauger**[p] **K.S. McFarland**[g] **J. Miller**[m] **J.G. Morfín**[h] **D. Naples**[c] **J.K. Nelson**[d] **C. Nguyen**[b] **G.N. Perdue**[h,g] **M.A. Ramírez**[p,k] **H. Ray**[b] **D. Ruterbories**[g] **C.J. Solano Salinas**[t] **H.M. Schellman**[a] **H. Su**[c] **M. Sultana**[g] **V.S. Syrotenko**[s] **N.H. Vaughan**[a] **A.V. Waldron**[u] **C. Wret**[g] **B. Yaeggy**[m] **K. Yang**[q] **L. Zazueta**[d]

[a] *Department of Physics, Oregon State University, Corvallis, Oregon 97331, USA*

[b] *University of Florida, Department of Physics, Gainesville, FL 32611*

[c] *Department of Physics and Astronomy, University of Pittsburgh, Pittsburgh, Pennsylvania 15260, USA*

[d] *Department of Physics, College of William & Mary, Williamsburg, Virginia 23187, USA*

[e] *AMU Campus, Aligarh, Uttar Pradesh 202001, India*

[f] *Sección Física, Departamento de Ciencias, Pontificia Universidad Católica del Perú, Apartado 1761, Lima, Perú*

[g] *University of Rochester, Rochester, New York 14627 USA*

[h] *Fermi National Accelerator Laboratory, Batavia, Illinois 60510, USA*

[k] *Campus León y Campus Guanajuato, Universidad de Guanajuato, Lascurain de Retana No. 5, Colonia Centro, Guanajuato 36000, Guanajuato México.*

[i] *University of Geneva, 1211 Geneva 4, Switzerland*

[j] *Centro Brasileiro de Pesquisas Físicas, Rua Dr. Xavier Sigaud 150, Urca, Rio de Janeiro, Rio de Janeiro, 22290-180, Brazil*

[l] *Department of Physics, University of Notre Dame, Notre Dame, Indiana 46556, USA*

[m] *Departamento de Física, Universidad Técnica Federico Santa María, Avenida España 1680 Casilla 110-V, Valparaíso, Chile*

[n] *York University, Department of Physics and Astronomy, Toronto, Ontario, M3J 1P3 Canada*
[o] *Department of Physical Sciences, IISER Mohali, Knowledge City, SAS Nagar, Mohali - 140306, Punjab, India*
[p] *Department of Physics and Astronomy, University of Pennsylvania, Philadelphia, PA 19104*
[q] *Oxford University, Department of Physics, Oxford, OX1 3PJ United Kingdom*
[r] *Massachusetts College of Liberal Arts, 375 Church Street, North Adams, MA 01247*
[s] *Physics Department, Tufts University, Medford, Massachusetts 02155, USA*
[t] *Facultad de Ciencias, Universidad Nacional de Ingeniería, Apartado 31139, Lima, Perú*
[u] *The Blackett Laboratory, Imperial College London, London SW7 2BW, United Kingdom*

Abstract: Charged-current neutrino interactions with low hadronic recoil ("low-ν") have a cross-section that is approximately constant versus neutrino energy. These interactions have been used to measure the shape of neutrino fluxes as a function of neutrino energy at accelerator-based neutrino experiments such as CCFR, NuTeV, MINOS and MINERvA. In this paper, we demonstrate that low-ν events can be used to measure parameters of neutrino flux and detector models and that utilization of event distributions over the upstream detector face can discriminate among parameters that affect the neutrino flux model. From fitting a large sample of low-ν events obtained by exposing MINERvA to the NuMI medium-energy beam, we find that the best-fit flux parameters are within their *a priori* uncertainties, but the energy scale of muons reconstructed in the MINOS detector is shifted by 3.6% (or 1.8 times the *a priori* uncertainty on that parameter). These fit results are now used in all MINERvA cross-section measurements, and this technique can be applied by other experiments operating at MINERvA energies, such as DUNE.

Contents

1 Introduction

Precise prediction of the neutrino flux from accelerator-based neutrino beams is a critical ingredient in neutrino physics. For example, the extraction of neutrino oscillation parameters in long-baseline neutrino experiments requires detailed simulations of reconstructed energy spectra, and neutrino flux predictions are the starting point of these simulations. Measurements of neutrino interaction cross-sections and other parameters in near detectors rely even more heavily on neutrino flux predictions, as they cannot take advantage of the experimental tuning of the flux model via the near detector used in long-baseline measurements.

The accelerator-based neutrino community has built a toolbox for improving flux predictions and estimating their uncertainties. This toolbox includes use of external hadron production data [1, 2] as well as measurements made in neutrino detectors. The latter is challenging because measurement of neutrino fluxes with a neutrino detector requires a "standard-candle" process with a known neutrino cross-section, and few-GeV neutrino cross-sections are generally poorly known. Neutrino scattering on electrons, a precisely calculable electroweak process, is one such standard candle, but because the final state electron energy is weakly correlated with the incoming neutrino energy, it constrains the flux normalization but provides little information about the shape of the flux versus energy.

Charged-current neutrino-nucleus scattering with low hadronic recoil ("low-ν") is another process that has been used as a standard candle. The inclusive ν_μ charged-current cross-section can be expressed as:

$$\frac{\mathrm{d}\sigma}{\mathrm{d}\nu} = \frac{G_F^2 M}{\pi}\int_0^1 \left(F_2 - \frac{\nu}{E_\nu}\left[F_2 + xF_3\right] + \frac{\nu}{2E_\nu^2}\left[\frac{Mx(1-R_L)}{1+R_L}F_2\right] + \frac{\nu^2}{2E_\nu^2}\left[\frac{F_2}{1+R_L} + xF_3\right]\right)\mathrm{d}x,$$

where E_ν is the neutrino energy, ν is the energy transferred from the neutrino to the hadronic final state, x is the Bjorken scaling variable, G_F is the Fermi constant, M is the struck nucleon's mass, F_2 and xF_3 are structure functions, and R_L is the structure function ratio $F_2/(2xF_1)$ [3]. In the limit that ν/E_ν is small, all of the energy-dependent terms in the equation above vanish, and the cross-section becomes a constant that is independent of energy. Although the absolute cross-section for this process is not well known, the fact that it is expected to be independent of neutrino energy means that it can be used to measure the shape of the neutrino flux. MINOS [4], and MINERvA [3, 5] have used this process to extract the neutrino energy spectrum of the Low Energy (LE) configuration of the Neutrinos at the Main Injector (NuMI) beam [6].

In this paper, we take the low-ν method a step further and use events with low hadronic energy to identify specific aspects of the flux and detector models that may be inaccurate. We further use the spatial distribution of low-ν events across the face of the detector to disentangle various effects. This technique is applicable to other on-axis neutrino experiments operating at similar energies, and could be exploited in detectors which take data at multiple off-axis locations, such as DUNE-PRISM [7]. The paper is organized as follows. Section 2 describes the MINERvA detector and simulation; Section 3 describes the reconstruction of low-ν events in the MINERvA detector. Fits to the spectra are described in Section 4 and conclusions are presented in Section 5.

2 MINERvA Experiment and Simulation

The MINERvA detector [8] is composed of 208 hexagonal planes of plastic scintillator interspersed with other materials. Each plane contains 127 1.7x3.3 cm triangular scintillator strips, arrayed in one of three directions to facilitate three-dimensional track and shower reconstruction. This study uses muon neutrino interactions in the inner tracker region, which is composed entirely of plastic scintillator planes. The tracker is surrounded at its outer edges and on the downstream end by scintillator planes separated by 0.2 cm-thick lead sheets, called the electromagnetic calorimeter (ECAL). Surrounding and downstream of the ECAL is a hadronic calorimeter (HCAL) composed of scintillator interspersed with steel. The upstream portion of MINERvA contains scintillator interspersed with passive targets made of carbon, iron, lead, water, and helium. This region was designed for comparing cross-sections across different nuclei and is not used for this study. The MINERvA detector is positioned 2 m upstream of the magnetized MINOS near detector, which is used to analyze the charge and momentum of muons exiting the back of MINERvA.

MINERvA is approximately on-axis in the NuMI beamline; the beamline is described in detail in Ref. [6]. NuMI begins with a 120 GeV proton beam, which is directed onto a 2-interaction length graphite target. The produced pions and kaons are focused using two parabolic focusing horns after which they decay in a 675 m long decay pipe. The MINERvA detector sits 1032 m downstream of the first focusing horn and is offset from the beam center by -56 cm in the x direction and -53 cm in the y direction where x is

left-right and y is top-bottom[1]. Data for this study were taken between September 9,2013 and February 6,2015. During this period NuMI was configured to focus positively charged particles, resulting in a primarily muon neutrino beam. NuMI was operated in the ME (Medium Energy) configuration, where the target began 1.43 m upstream of the front face of the first focusing horn and the second horn was 21 m downstream of the first horn. The focusing peak of the muon neutrino flux in this configuration was approximately 6 GeV.

Simulated MINERvA data begins with a Geant4 simulation of the NuMI beamline. We use g4numi version v6r3, based on Geant4 version 4.9.3p6 with the FTFP_BERT physics list. The beam simulation is corrected with data from hadron production measurements [1].

Neutrino interactions in the MINERvA detector are simulated using the GENIE [9, 10] event generator version 2.12.6. Within this framework, Quasi-elastic events are simulated using the Llewellyn-Smith formalism [11] with BBBA05 [12] and a dipole axial form factor with axial mass of 0.99 GeV; resonant pion production uses the Rein-Sehgal model [13] with an axial mass of 1.12 GeV; deep inelastic scattering uses the Bodek-Yang model [14]. The initial state nuclear model uses a Relativistic Fermi Gas [15] with an additional high momentum tail as prescribed by Bodek and Ritchie [16]. Final state interactions of hadrons following the initial hard scatter are simulated using the INTRANUKE h-A model [17].

MINERvA makes several modifications to the base GENIE model that are collectively known as MINERvA tune v1. These modifications are as follows:

- Low-Q^2 quasi-elastic interactions are modified using The Valencia [18] RPA description, as described in [19].
- Valencia model [20–22] two-particle, two-hole (2p2h) events are added to the GENIE base model and enhanced using a fit to MINERvA inclusive data [23, 24].
- Non-resonant pion production is suppressed to 40% of its original strength based on a re-analysis of bubble chamber data [25].

The response of the MINERvA detector is simulated using Geant4 version 4.9.3p6 with the QGSP_BERT physics list validated with measurements using a scaled-down version of the detector operated in a hadron test beam [26]. The MINERvA readout and calibration are simulated as described in Ref. [8]. Overlapping events (pile-up) are simulated by overlaying randomly sampled data spills on generated Monte Carlo events, scaled appropriately to simulate different periods of intensity during the running.

3 Low-ν Event Reconstruction

The MINERvA detector collects charge depositions (hits) throughout each 10 μs NuMI spill. After being read out and calibrated as described in Ref. [8], the hits are correlated

[1]We use the beam coordinate system where the z axis points downstream along the center of the beam, the y axis points upward, and the x axis is horizontal pointing to beam left.

in time into so-called time slices. These are collections of hits consistent with energy depositions from a single neutrino interaction. Within each time slice, a Kalman filter is used to identify tracks in both the MINERvA and MINOS detectors. Tracks in the two detectors are then matched based on both time and spatial information. These matched tracks are deemed to be muons, the only particles capable of producing tracks in both detectors. To estimate the energy of the non-muon hadronic recoil system, all other hits in MINERvA that are not on the muon track are grouped together and corrected for passive material and neutral particle content using the Monte Carlo simulation described in section 2. For the purposes of this study, events are deemed to be low-ν if the hadronic recoil is less than 800 MeV.

An estimate of neutrino energy is formed by summing the muon energy and the hadronic recoil energy. The muon energy is derived from the range in MINERvA combined with range in MINOS for muons stopping in MINOS or based on bend in the MINOS magnetic field otherwise. The distribution of neutrino energy in data and the simulation is shown in figure 1, with the simulation both absolutely normalized (left) and area-normalized to the same number of events as data (right). A significant discrepancy between the data and simulation is apparent.

The simulated distribution is subject to a number of systematic uncertainties. All of these have been described in previous MINERvA publications, so we mention them briefly here and include references with more detail on how they are assessed.

- Neutrino flux uncertainties, arising from models of hadron production in the target and other beamline materials, as well as accuracy of the simulated beam and focusing system [1].
- GENIE interaction model uncertainties, arising from both final state and primary interaction models [9, 10].
- Additional model-related uncertainties assessed on the MINERvA modifications to GENIE [24].
- Uncertainties in the hadronic response of the MINERvA detector [27].
- Uncertainties associated with reconstruction of muon tracks in MINERvA and MINOS [27].

A summary of the fractional uncertainty due to each of these sources as a function of neutrino energy is shown in figure 2. The largest uncertainties are associated with the GENIE interaction model.

Ratios of data and Monte Carlo are shown in figure 3. There is a discrepancy between data and simulation that varies substantially as a function of energy. While this discrepancy is well-covered by the systematic uncertainties, the shape of the discrepancy is much larger than the shape-only component of the systematic uncertainty shown in the right of

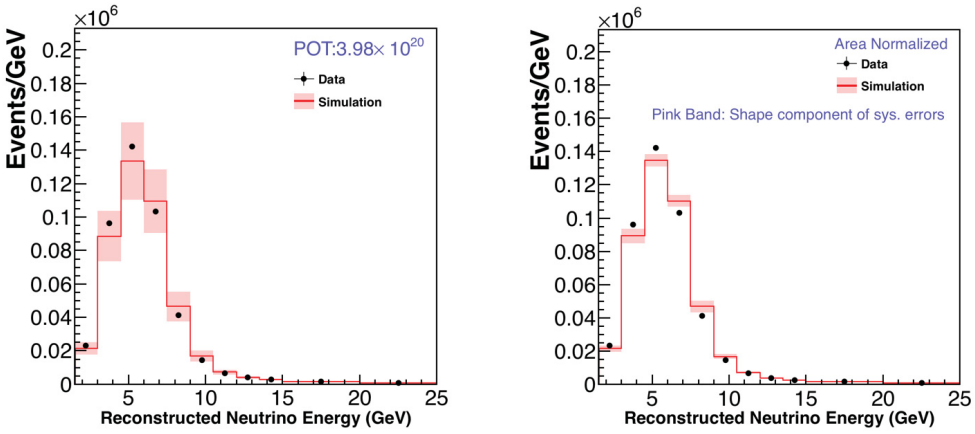

Figure 1. Distribution of reconstructed neutrino energy in low-ν events in MINERvA data and simulation. Data and simulated low-ν events with absolute normalization are shown in the left plot. The right plot shows the area normalized data and simulated low-ν events. The pink band is the systematic uncertainties on simulated events.

figure 3. Most of the sources of systematic uncertainty described above primarily affect the normalization of the low-ν spectrum but not the shape. However, there are two sources of uncertainty that could cause discrepancies similar to that shown in figure 3, namely 1) beam focusing parameters and 2) the muon energy scale. The hadronic energy scale can also modify the shape of the low-ν spectrum, but because it comprises a very small component of the neutrino energy, it cannot fully account for this discrepancy. To better understand the source of the discrepancy, fits to the neutrino energy were performed that allowed focusing and muon energy parameters to vary.

4 Fits to Energy Spectra

Several known sources of uncertainty in MINERvA's simulation can cause a shift in the energy spectrum similar to the discrepancy seen in Figure 3. These include the muon energy scale, which makes up the bulk of the reconstructed neutrino energy in these events. Another potential source of the shift is neutrino beam alignment parameters, which preferentially affect high-energy hadrons that skim the inner edge of the focusing horns and can cause distortions at the falling edge of the neutrino flux focusing peak. Beam alignment tolerances are shown in table 1, and the ratio of predicted neutrino flux with these parameters shifted by one standard deviation to the nominal flux is shown in figure 4. Shifts of several quantities can create distortions in the predicted neutrino energy spectrum between 5-15 GeV. These include the Horn 1 transverse position, the horn current, the size of the horn water layer, and the proton beam position. However, the shape of the

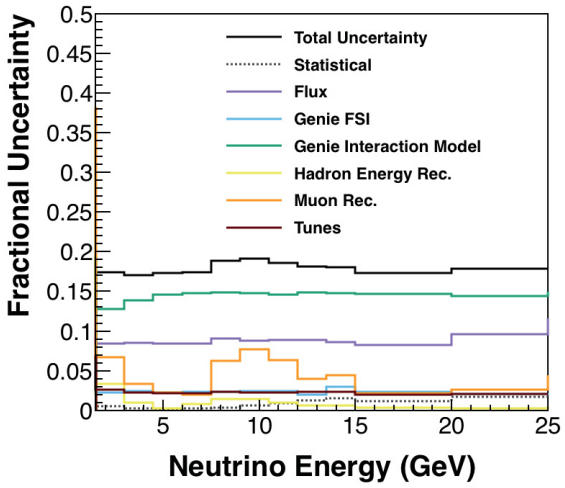

Figure 2. Summary of fractional systematic uncertainties on the simulated neutrino energy distribution for low-ν events shown in figure 1.

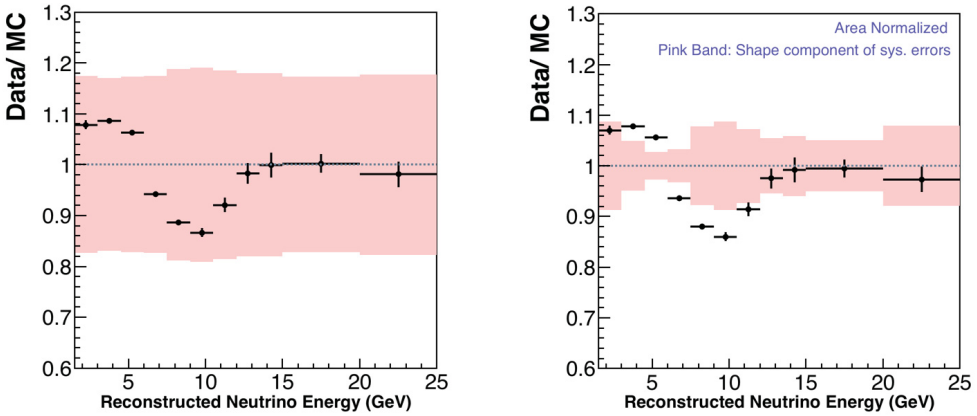

Figure 3. Ratio of the data and simulation for the low-ν distribution before the fits described in section 4, both absolutely normalized (left) and with data and simulation normalized to the same number of events (right). The pink band is the systematic error band for the simulation, with only the shape component of the systematic uncertainty shown in the right plot.

Parameter	Nominal Value	1 σ shift from Nominal Value
Beam Position (X)	0 mm	1 mm
Beam Position (Y)	0 mm	1 mm
Beam Spot Size	1.5 mm	0.3 mm
Horn Water Layer	1.0 mm	0.5 mm
Horn Current	200 kA	1 kA
Horn 1 Position (X)	0 mm	1 mm
Horn 1 Position (Y)	0 mm	1 mm
Horn 1 Position (Z)	30 mm	2 mm
Horn 2 Position (X)	0 mm	1 mm
Horn 2 Position (Y)	0 mm	1 mm
Target Position (X)	0 mm	1 mm
Target Position (Y)	0 mm	1 mm
Target Position (Z)	-1433 mm	1 mm
POT Counting	0	0.02% of Total POT
Baffle Scraping	0	0.25% of POT

Table 1. Beam Parameters that are used in the MINERνA Medium Energy run configuration.

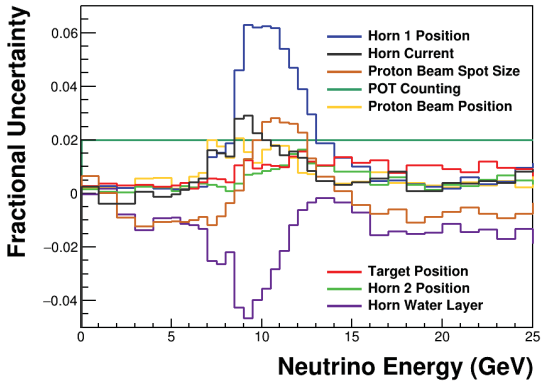

Figure 4. Ratio of predicted neutrino flux with beam parameters shifted by one standard deviation (see table 1) to the nominal neutrino flux.

discrepancy within this region and the magnitude per standard deviation vary among the parameters.

The beam focusing parameters can be further differentiated by taking advantage of the fact that transverse shifts in beam parameters affect various regions of the detector differently. To further understand this effect, the low-ν event sample was separated according to transverse vertex position within the MINERvA detector using the seven bins shown in figure 5. The radius of the NuMI beam is larger than the MINERvA detector, so the flux is nearly constant over the face of the detector. However, the beam is small enough in size

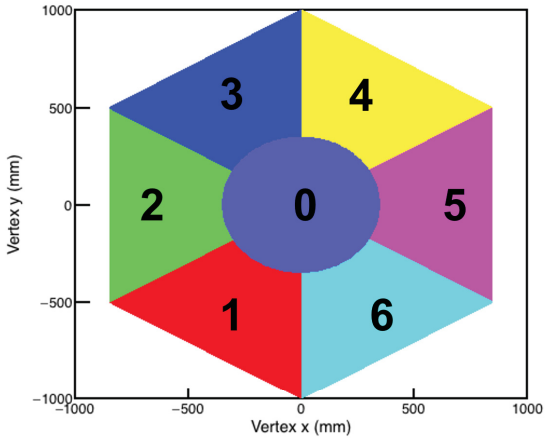

Figure 5. The seven bins of interaction vertex transverse position used for the fits to low-ν neutrino energy spectra.

that shifts of certain beam parameters from their nominal positions cause variations in flux that are not constant across the detector. Changes in flux under variations of two alignment parameters are shown in figure 6. In general, transverse shifts to beam components such as the primary proton beam or the horns create different effects in each of the vertex bins, while other types of shifts create a uniform effect in all bins.

The ratios of data to simulation of the low-ν neutrino energy spectra in each of these bins are shown in figure 7. The discrepancy is broadly similar in each bin, indicating that the mismodeling is not consistent with a transverse shift of a beam component.

To further understand which parameters could be the source of the discrepancy, a fit was performed to the low-ν neutrino energy spectra allowing the beam focusing parameters given in table 1[2] and the MINOS muon energy scale[3] to vary. In addition to those parameters that primarily affect the shape of the spectrum, the overall normalization of the spectrum was also allowed to float. The fit minimized a chi squared defined as:

$$\chi^2 = \sum_{ij} \frac{(Data'_{ij} - MC'_{ij})^2}{\sigma^2_{ij}}$$

where $Data'_{ij}$ (MC'_{ij}) is the number of events in the data (simulation) in the ith energy bin and the jth vertex bin under some set of varied parameters. The sum is over nine

[2]A parameter for baffle scraping was omitted from the fit, since this parameter has a negligible impact on the predicted neutrino flux

[3]The total muon energy combines the muon energy as reconstructed in MINOS with an estimate of energy loss in the MINERvA detector prior to entering MINOS. The MINERvA component of the energy is small, and the fit was found to be insensitive to variations in the energy scale within MINERvA, so only the MINOS component of the energy was varied in the fits.

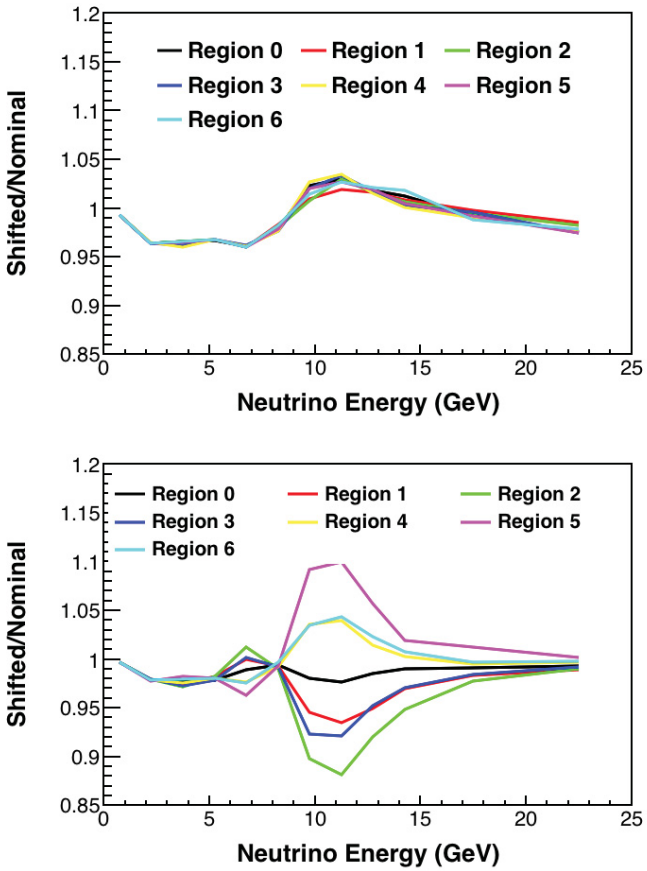

Figure 6. Ratio of varied to nominal neutrino flux for 1 σ shifts in the primary proton beam spot size (top) and transverse position on target (bottom), in the seven vertex position bins shown in figure 5.

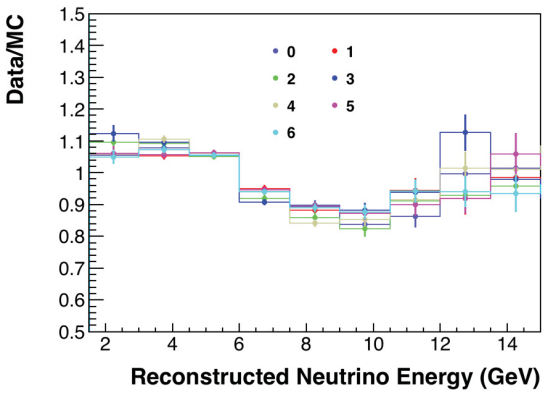

Figure 7. Ratio of low-ν data to simulation in the seven vertex position bins shown in figure 5.

energy bins between 1.5 and 15.0 GeV and the seven vertex bins of figure 5. The data and simulated events are reweighted by the flux prediction based on the muon energy scale shift (for data) and focusing parameters (for simulated events).

The uncertainty is the combined statistical uncertainty of the data and simulation:

$$\sigma_{ij}^2 = \sqrt{\sigma_{Data',ij}^2 + \sigma_{MC'_{ij}}^2}.$$

Fits were performed both with the above χ^2 and with a modified χ^2 that added a penalty term based on the prior uncertainty on each of the parameters:

$$\chi^2_{prior} = \sum_{ij} \frac{(Data'_{ij} - MC'_{ij})^2}{\sigma_{ij}^2} + \sum_k (\alpha_k)^2,$$

where α_k is the number of standard deviations that parameter k has been shifted from its nominal value. The standard deviations are taken from the nominal beam parameter tolerances given in table 1 except for the longitudinal position of the target, for which the prior was conservatively increased to 3 mm.

The result of the fits to the data/simulation ratio is shown in figure 8, while the best fit parameters from the fit are shown in table 2, along with their statistical and systematic uncertainties. Systematic uncertainties on the fit parameters were assessed by shifting underlying parameters (described in section 3), repeating the fit, and taking the difference between the best fit parameter in the nominal and shifted fits as a systematic uncertainty on the parameter. All such systematic uncertainties are added in quadrature to estimate the systematic uncertainties quoted in table 2.

In both versions of the fit (with and without prior assumptions), the simulation agrees substantially better with the data. The bulk of the improvement arises from the MINOS muon energy scale, which is shifted by 3.6% (1.8 times the *a priori* standard deviation of this parameter). All other parameters are consistent within uncertainties with less than one standard deviation shift from their nominal values, with the exception of the target y position, which is pulled by nearly two standard deviations, but has a very modest impact on the predicted neutrino flux.

The 2% *a priori* uncertainty on the MINOS muon energy scale is due to underlying uncertainties in the detector mass and in models of the detector geometry and muon energy loss used in the simulation [28]. It was validated with scaled down versions of the MINOS detector [29] and constitutes the total muon energy uncertainty for muons reconstructed by range. For muons reconstructed by curvature, MINERvA adds an additional uncertainty of 0.6%(2.5%) for muons greater than (less than) 1 GeV, based on comparisons of energies reconstructed by range and curvature for tracks where both reconstructions are possible. Alternative versions of the fit were performed adding extra degrees of freedom for the energy scale of muons reconstructed by curvature, but the fit was found to be insensitive to these parameters.

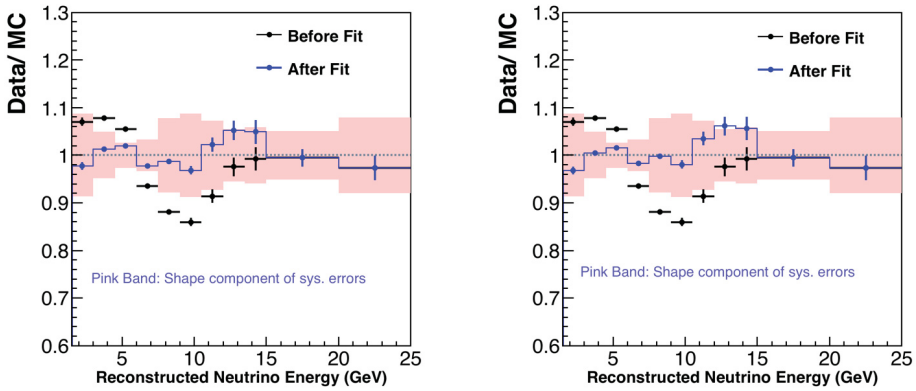

Figure 8. Ratio of low-ν events in data and simulation before (black) and after (blue) the fits that did not (left) and did (right) include a prior penalty term. The data and simulation are normalized to the same number of events. The error bars are statistical errors. The pink band shows the shape component of the systematic uncertainty on the ratio.

Parameter	Nominal	Best Fit (No Prior)	Best Fit (Prior)
Beam Position (X)	0.0 mm	$-0.3 \pm 0.3 \pm 0.1$ mm	$-0.3 \pm 0.2 \pm 0.1$ mm
Beam Position (Y)	0.0 mm	$0.8 \pm 0.3 \pm 0.3$ mm	$0.7 \pm 0.2 \pm 0.2$ mm
Target Position (X)	0.0 mm	$-0.8 \pm 0.3 \pm 0.1$ mm	$-0.8 \pm 0.3 \pm 0.1$ mm
Target Position (Y)	0.0 mm	$2.3 \pm 0.7 \pm 1.2$ mm	$1.7 \pm 0.6 \pm 0.8$ mm
Target Position (Z)	-1433 mm	$-1432.4 \pm 2.4 \pm 0.3$ mm	$-1431 \pm 1.8 \pm 0.3$ mm
Horn 1 Position (X)	0.0 mm	$-0.3 \pm 0.4 \pm 0.5$ mm	$-0.1 \pm 0.3 \pm 0.1$ mm
Horn 1 Position (Y)	0.0 mm	$0.1 \pm 0.5 \pm 0.5$ mm	$0.0 \pm 0.3 \pm 0.3$ mm
Beam Spot Size	1.5 mm	$1.41 \pm 0.09 \pm 0.03$ mm	$1.32 \pm 0.09 \pm 0.03$ mm
Horn Water Layer	1.0 mm	$1.2 \pm 0.3 \pm 0.05$ mm	$1.3 \pm 0.25 \pm 0.1$ mm
Horn Current	200 kA	$198.0 \pm 1.4 \pm 1.4$ kA	$199.1 \pm 0.7 \pm 0.5$ kA
Muon Energy Scale	1.0	$1.032 \pm 0.004 \pm 0.008$	$1.036 \pm 0.004 \pm 0.006$

Table 2. Shift of beam parameters from the fits with and without priors.

To further investigate the fit conclusions, a fit was also performed allowing only beam parameters (and not muon energy scale) to vary. The results of those fits are available in table 3. This alternative fit also achieves good agreement with data and simulation, but results in a shift to the target longitudinal position by 13.6 mm, or more than ten times its 1 mm tolerance. NuMI beam experts are confident that the target position was within its tolerance.

MINERvA has also used neutrino-electron scattering to constrain the neutrino flux prediction [30]. However, that data is primarily sensitive to the normalization of the flux, not the shape, and that data is consistent both with the *a priori* flux prediction and with the

Parameter	Nominal Value	New Value
Beam Position (X)	0 mm	-0.2 ± 0.12 mm
Beam Position (Y)	0 mm	-0.53 ± 0.14
Beam Spot Size	1.5 mm	1.22 ± 0.14 mm
Horn Water Layer	1 mm	0.895 ± 0.16 mm
Horn Current	200 kA	197.41 ± 0.76 kA
Horn 1 Position (X)	0 mm	0. ± 0.17 mm
Horn 1 Position (Y)	0 mm	-0.39 ± 0.17 mm
Target Position (X)	0 mm	-0.32 ± 0.17 mm
Target Position (Y)	0 mm	1.65 ± 0.5 mm
Target Position (Z)	-1433 mm	-1419.44 ± 1.83 mm

Table 3. Prior and best-fit beam parameters from an alternative fit that did not include the MINOS muon energy scale as a fit parameter.

flux model using all fit results described here.

Since a shift of the MINOS muon energy scale of 1.8 standard deviations is substantially more likely than a shift in the target position of more than 10 standard deviations, we attribute this discrepancy to the MINOS muon energy scale. For all MINERvA analyses using this data set, the MINOS muon energy scale in the data is shifted by 3.6%. Since the flux predicted by the nominal fit is consistent with the *a priori* flux within uncertainties, no correction is made to the flux model. Because the muon energy is reconstructed primarily using the MINOS near detector, other energy quantities reconstructed in MINERvA events, such as hadronic recoil energy, are presumably not affected, and are not corrected. Figure 9 shows that a shift of 1.8 σ removes the discrepancy between the data and simulation.

5 Conclusion

The MINERvA collaboration has analyzed a sample of charged current muon neutrino interactions with low hadronic recoil. A significant discrepancy between data and simulation was observed in the shape of the reconstructed neutrino energy spectrum in this sample. The discrepancy is consistent with a mismodeling of the alignment parameters of the neutrino beam or of the detector energy scale. Fits to this data allowing various parameters in the simulation to vary indicate that the discrepancy is most consistent with a 3.6% shift to the MINOS muon energy scale. Based on this work, measurements of neutrino cross-sections using this MINERvA dataset include a correction to the MINOS muon energy scale. This work follows earlier uses of low-ν samples to measure neutrino flux, but is the first time that this sample has been use to investigate specific sources of neutrino flux and detector mismodeling. The procedure described here to fit reconstructed low-ν spectra to flux and detector parameters could be used by other accelerator-based neutrino experiments operating at similar energies. Additionally, in detectors where the

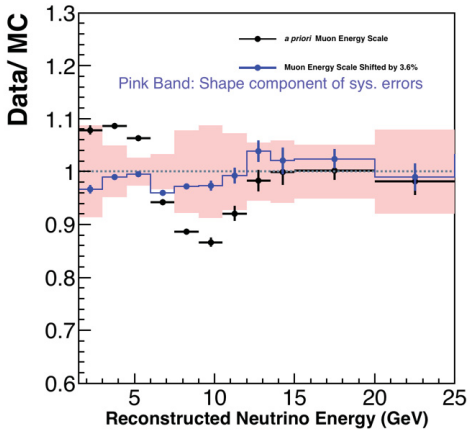

Figure 9. Ratio of low-ν data to MC with the muon energy scale at its nominal value (black) and with the muon energy scale shifted by 3.6% from its nominal value (blue) as prescribed by the fit and adopted by the collaboration. The data and simulation are normalized to the same number of events. The error bars are statistical errors. The pink band shows the shape component of the systematic uncertainty.

size of the neutrino beam and neutrino detector are similar, the use of transverse vertex position can be used to increase the efficacy of this technique.

Acknowledgments

This document was prepared by members of the MINERvA Collaboration using the resources of the Fermi National Accelerator Laboratory (Fermilab), a U.S. Department of Energy, Office of Science, HEP User Facility. Fermilab is managed by Fermi Research Alliance, LLC (FRA), acting under Contract No. DE-AC02-07CH11359. These resources included support for the MINERvA construction project, and support for construction also was granted by the United States National Science Foundation under Award No. PHY-0619727 and by the University of Rochester. Support for participating scientists was provided by NSF and DOE (USA); by CAPES and CNPq (Brazil); by CoNaCyT (Mexico); by Proyecto Basal FB 0821, CONICYT PIA ACT1413, and Fondecyt 3170845 and 11130133 (Chile); by CONCYTEC (Consejo Nacional de Ciencia, Tecnología e Innovación Tecnológica), DGI-PUCP (Dirección de Gestión de la Investigación - Pontificia Universidad Católica del Peru), and VRI-UNI (Vice-Rectorate for Research of National University of Engineering) (Peru); NCN Opus Grant No. 2016/21/B/ST2/01092 (Poland); by Science and Technology Facilities Council (UK). We thank the MINOS Collaboration for use of its near detector data. Finally, we thank the staff of Fermilab for support of the beam line, the detector, and computing infrastructure.

References

[1] L. Aliaga *et al.* (MINERvA Collaboration), Phys. Rev. D **94**, 092005 (2016), [Addendum: Phys. Rev. D **95**, no.3, 039903 (2017)], arXiv:1607.00704 .

[2] K. Abe *et al.* (T2K), Phys. Rev. D **87**, 012001 (2013), [Addendum: Phys. Rev. D **87**, no. 1, 019902 (2013)], arXiv:1211.0469 [hep-ex] .

[3] J. Devan *et al.* (MINERvA), Phys. Rev. D **94**, 112007 (2016), arXiv:1610.04746 [hep-ex] .

[4] P. Adamson *et al.* (MINOS), Phys. Rev. D **81**, 072002 (2010), arXiv:0910.2201 [hep-ex] .

[5] L. Ren *et al.* (MINERvA), Phys. Rev. D **95**, 072009 (2017), [Addendum: Phys. Rev.D **97**, no. 1, 019902 (2018)], arXiv:1701.04857 [hep-ex] .

[6] P. Adamson *et al.*, Nucl. Instrum. Meth. A **806**, 279 (2016), arXiv:1507.06690 .

[7] B. Abi *et al.* (DUNE), Deep Underground Neutrino Experiment (DUNE), Far Detector Technical Design Report, Volume II DUNE Physics (2020), arXiv:2002.03005 [hep-ex] .

[8] L. Aliaga *et al.* (MINERvA Collaboration), Nucl. Instrum. Meth. A **743**, 130 (2014), arXiv:1305.5199 .

[9] C. Andreopoulos *et al.* (GENIE Collaboration), Nucl. Instrum. Meth. A **614**, 87 (2010), arXiv:0905.2517 [hep-ph] .

[10] C. Andreopoulos, C. Barry, S. Dytman, H. Gallagher, T. Golan, R. Hatcher, G. Perdue, and J. Yarba, (2015), arXiv:1510.05494 .

[11] C. H. Llewellyn Smith, *Gauge Theories and Neutrino Physics, Jacob, 1978:0175*, Phys. Rept. **3**, 261 (1972).

[12] R. Bradford, A. Bodek, H. S. Budd, and J. Arrington, Nucl. Phys. Proc. Suppl. **159**, 127 (2006), arXiv:hep-ex/0602017 [hep-ex] .

[13] D. Rein and L. M. Sehgal, Annals of Physics **133**, 79 (1981).

[14] A. Bodek, I. Park, and U.-K. Yang, Nucl. Phys. Proc. Suppl. **139**, 113 (2005), arXiv:hep-ph/0411202 [hep-ph] .

[15] R. S. and E.J. Moniz, Nucl. Phys. B **43**, 605 (1972).

[16] A. Bodek and J. L. Ritchie, Phys. Rev. D **24**, 1400 (1981).

[17] S. Dytman, AIP Conf. Proc. **896**, 178 (2007), [,178(2007)].

[18] J. Nieves, J. E. Amaro, and M. Valverde, Phys. Rev. C **70**, 055503 (2004), [Erratum: Phys. Rev.C 72,019902(2005)], arXiv:nucl-th/0408005 .

[19] R. Gran, (2017), arXiv:1705.02932 .

[20] J. Nieves, I. Ruiz Simo, and M. Vicente Vacas, Phys. Rev. C **83**, 045501 (2011), arXiv:1102.2777 [hep-ph] .

[21] R. Gran, J. Nieves, F. Sanchez, and M. Vicente Vacas, Phys. Rev. D **88**, 113007 (2013), arXiv:1307.8105 [hep-ph] .

[22] J. Schwehr, D. Cherdack, and R. Gran, (2016), arXiv:1601.02038 [hep-ph] .

[23] P. A. Rodrigues *et al.* (MINERvA), Phys. Rev. Lett. **116**, 071802 (2016), arXiv:1511.05944 [hep-ex] .

[24] D. Ruterbories *et al.* (MINERvA Collaboration), Phys. Rev. D **99**, 012004 (2019), arXiv:1811.02774 .

[25] P. Rodrigues, C. Wilkinson, and K. McFarland, Eur. Phys. J. C **76**, 474 (2016), arXiv:1601.01888 [hep-ex] .

[26] L. Aliaga *et al.* (MINERvA Collaboration), Nucl. Instrum. Meth. A **789**, 28 (2015), arXiv:1501.06431 [physics.ins-det] .

[27] J. Mousseau *et al.* (MINERvA), Phys. Rev. D **93**, 071101 (2016), arXiv:1601.06313 [hep-ex] .

[28] D. Michael, P. Adamson, T. Alexopoulos, W. Allison, G. Alner, K. Anderson, C. Andreopoulos, M. Andrews, R. Andrews, C. Arroyo, and et al., Nuclear Instruments and Methods in Physics Research Section A: Accelerators, Spectrometers, Detectors and Associated Equipment **596**, 190–228 (2008).

[29] P. Adamson, G. Crone, L. Jenner, R. Nichol, R. Saakyan, C. Smith, J. Thomas, M. Kordosky, K. Lang, P. Vahle, A. Belias, T. Nicholls, G. Pearce, D. Petyt, M. Barker, A. Cabrera, J. Hartnell, P. Miyagawa, N. Tagg, A. Weber, E. Falk Harris, P. Harris, R. Morse, P. Symes, D. Michael, P. Litchfield, R. Lee, and S. Boyd, Nuclear Instruments and Methods in Physics Research Section A: Accelerators, Spectrometers, Detectors and Associated Equipment **556**, 119 (2006).

[30] E. Valencia *et al.* (MINERvA), Phys. Rev. D **100**, 092001 (2019), arXiv:1906.00111 [hep-ex] .